Article

Not peer-reviewed version

The Effect of Carbon Nanotubes and Carbon Micro Fibers on the Piezoresistive and Mechanical Properties of Mortar

Irene Kanellopoulou *, Ioannis A. Kartsonakis *, Evangelia K. Karaxi , Athanasia I. Chrysanthopoulou , Costas A. Charitidis

Posted Date: 13 June 2024

doi: 10.20944/preprints202406.0937.v1

Keywords: carbon micro fibers; carbon nanotubes; cement; piezoresistive; flexural strength; compressive strength

Article

The Effect of Carbon Nanotubes and Carbon Micro Fibers on the Piezoresistive and Mechanical Properties of Mortar

Irene Kanellopoulou [1,*], Ioannis A. Kartsonakis [1,2,*], Evangelia K. Karaxi [1], Athanasia I. Chrysanthopoulou [1] and Costas A. Charitidis [1]

[1] Research Unit of Advanced, Composite, Nano-Materials and Nanotechnology, School of Chemical Engineering, National Technical University of Athens, 9 Heroon Polytechniou St., Zographos, GR-15773 Athens, Greece; ikan@chemeng.ntua.gr (I.A.K.); dcar@chemeng.ntua.gr (E.K.K.); athanasiachrysanthopoulou@gmail.com (A.I.C.); charitidis@chemeng.ntua.gr (C.A.C.)

[2] Physical Chemistry Laboratory, School of Chemistry, Aristotle University of Thessaloniki, GR-54124, Thessaloniki, Greece; ikartson@chem.auth.gr (I.A.K)

* Correspondence: ikan@chemeng.ntua.gr (I.K.); ikartson@chem.auth.gr (I.A.K.); Tel.: +30-2310997817)

Abstract: In this study, the mechanical and piezoresistive properties of mortars reinforced with carbon nanotubes (CNTs) and carbon micro fibers (CMFs) are determined. Silica fume as well as a polymer with polyalkylene glycol graft chains were used as dispersant agents for the CNTs and CMFs incorporation into the cement paste. The mechanical properties of the mortar composites were investigated in respect to their flexural and compressive strength. A four-probe method was used for the estimation of their piezoresistive response. The test outcomes revealed that the combination of the dispersant agents along with a low content of CNTs and CMF by weight of cement (bwoc) result in the production of a stronger mortar with enhanced mechanical performance and durability. More specifically, there was an increase in flexural and compressive strength up to 38% and 88%, respectively. Moreover, the piezoresistive response of the reinforced cementitious materials was attributed to the variation of electrical resistivity due to tunneling transport of electrons stemming from two different mechanisms due to the incorporation of the conductive admixtures (CNTs and CMF). This work aims to contribute to the progress acceleration in the field of developing structural materials with self-sensing and electrical actuation related properties.

Keywords: carbon micro fibers; carbon nanotubes; cement; piezoresistive; flexural strength; compressive strength

 doi:10.20944/preprints202406.0937.v1

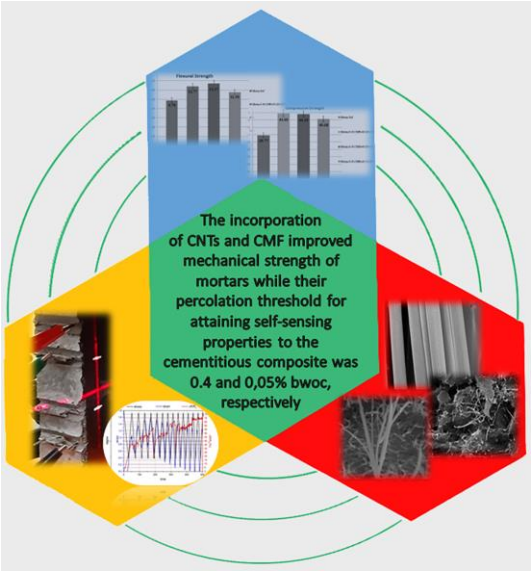

1. Introduction

Cementitious based materials are widely used in the construction engineering field due to their low cost, rich resources and high compressive strength. These materials are very popular because they can be easily produced, used locally and have a good environmental adjustability [1]. However, such constructions are subjected to deterioration due to erosion and corrosion processes. Therefore, cement composite materials are reinforced using several fillers such as carbon nanotubes (CNTs), carbon nanofibers (CNFs) and micro fibers (CMFs), inorganic nanoparticles, graphene oxides, etc. The incorporation of these fillers aims to the mechanical as well as electrical and thermal properties enhancement of the produced composite materials [2].

Carbon nanotubes are widely used as cement reinforcing materials because of their enhanced mechanical properties and carrying capacities due to the presence of sp^2 hybrid orbitals in their C atoms along with their high aspect ratio and fiberlike structure. They also exhibit high electrical conductivity which is attributed to the π C-C bonds on the z plane which can potentially reinforce the piezoresistive properties of cementitious materials containing them [3]. According to literature, embodied CNTs into concrete act as bridges across voids and cracks forming interfacial bonds with cement, thus resulting to the compressive strength improvement [4–6]. Similar outcomes have been observed in the studies of Haddad et al. [7], Li et al. [8] and Wang et al. [9]. The direct fabrication of CNTs on clinker so as to be employed in cement-based materials is also mentioned in literature by the group of Calixto [10]. In the work of Moon et al. [11] it is stated that the effective dispersion of CNTs in ultra-high performance concrete leads to on one hand, a remarkable enhancement of electrical conductivity and on the other hand, the formation of a denser structure with improved mechanical properties with respect to stiffness.

Carbon fibers are also widely used as fillers for cement composites due to their unique properties such as fatigue, creep, corrosion and high temperature resistance. Moreover, their chemical stability and electrical conductivity along with their light weight and high specific strength, enable the usage of CMFs as fillers in concrete. The work of Gao et al. reported that the mechanical properties of cement-based composites with respect to flexural strength are enhanced and the resistivity is decreased after the incorporation of CMFs [12]. Chuang et al. stated that the CMFs concentration influences the conductivity of cement-based composites [13]. The work of Diaz et al. indicated that the incorporation of short CMFs on cement paste outcomes to a resistance reduction [14]. In the research of Wang et al. it was revealed that both the bending strength and conductivity of cement-based composites are improved with better CMF distribution [15].

Over the last few years, both CNTs and CMFs have received increasing interest as fillers. The group of Lee et al. resulted that both CMFs and CNTs incorporation in cementitious composites

 doi:10.20944/preprints202406.0937.v1

improves the stability of the electrical resistivity of the composites [16]. The embodiment of them into cementitious based materials imparts improvement of their final mechanical properties with respect to flexural and compressive strength. Moreover, the electrical resistivity of the materials variates during a loading-unloading procedure, indicating material's sensing capability. In the work of Yoon et al. the synergistic effect of CMFs and CNTs that were added into cement composites was investigated in respect of the electromagnetic wave shielding properties [17].

However, an important factor that influences the final behavior of the cementitious based materials is the dispersion quality of the CNTs and CMFs into the matrix. Agglomerates of CNTs and CMFs are formed during the dispersion process due to their intrinsic hydrophobic surfaces. Thus, many attempts have been performed on the improvement of CNTs and CMFs dispersibility into cement composites. In literature, there are several studies reporting the employment of silica fume as dispersing agent for cement fillers such as CNTs and CMFs [18,19]. Silica fume can enhance the strength of concrete because of its chemical composition. It has been proved that concrete which contains silica fume can preserve its strength for a long time. The positive effect of silica fume is assigned to its spherical-shaped particles that penetrate into the cementitious composites and increase the distance between the fillers [20,21]. Kim et al. found that the incorporation of silica fume to the concrete eventuated to the enhancement of its mechanical and electrical properties because of the improvement of CNTs dispersion [22]. Stynoski et al. showcased that the use of silica fume enhanced the mechanical properties of mixtures containing CNTs and CMFs, denoting a stronger frictional bond between the reinforcement agent and the matrix [23]. In the work of Chuang et al. it was revealed that the addition of silica fume into cement-based composites effected positively the CMFs dispersion and was correlated to an increase of the electrical conductivity of the composites [13]. Furthermore, several other studies have proved that the addition of silica fume to either mortar or concrete resulted to an increase of the CNTs and CMFs dispersion which subsequently led to improved electrical and mechanical properties of the composites [24,25]. In the work of Song et al. it was revealed that the CNTs dispersibility into mortar was improved with increasing replacement ratio of silica fume [20]. The use of polycarboxylate-based stabilizers additionally provides a positive effect on the dispersibility of CNTs and CMFs into the cement paste without deteriorating or destroying their structure [26–29]. This type of stabilizers acts as effective dispersion agent because of their long lateral ether chains that impart steric repulsion between the fillers in the cement-based composites [30].

The motivation of the present work is the development of cementitious based composite materials with structural sensing and electrical actuation along with enhanced mechanical properties. The aim of this work is the identification of structural changes of mortar and the determination of properties enhancement inflicted by the incorporation of CNTs and CMFs together with silica fume. More specifically, their effect on the mechanical properties and electrical conductivity of the cementitious matrix as a function of their concentration is estimated. Mortar test specimens were prepared comprising a range of CNTs and CMFs concentrations, by weight of cement (bwoc). The surface morphology of the prepared as well as the fractured cement specimens was evaluated via SEM, while the elemental analysis was performed via energy dispersive x-ray analysis. The macro-mechanical integrity was investigated with respect to flexural and compressive strength (EN 196-1). The results revealed that the CNTs, CMFs and dispersing agent content influence the mechanical properties and electrical conductivity of the mortar specimens. Finally, it may be remarked that the added value of this work resides in the fact that the presented results shed light on the current and future opportunities to accelerate progress in the field of material development with structural sensing and electrical actuation.

2. Materials and Methods

2.1. Materials

Analytical reagent grade chemicals were used. Portland Cement CEM I 52.5 N was used as cementitious material; its physical properties and chemical composition are summarized in Table 1. Sand (NORMENSAND CEN-Standard Sand DIN EN 196-1) and silica fume (Sika® Silicoll P) were

 doi:10.20944/preprints202406.0937.v1

used as aggregates whereas SIKA SI100 (polymer with polyalkylene glycol polymer graft chains) was used as stabilizer. Multi-walled carbon nanotubes (CNTs) were fabricated through Catalytic Thermal Chemical Vapor Deposition method (CT-CVD) according to our previous works [31,32]. Finally, the CMFs were received from R&G Faserverbundwerkstoffe GmbH (chopped carbon fiber strands 3 mm).

Table 1. Chemical compositions and physical properties of cementitious materials*, **.

Composition	SiO_2	Al_2O_3	Fe_2O_3	CaO	MgO	SO_3	Na_2O	K_2O
% (mass) cement	19.47	4.75	3.43	63.16	1.43	2.68	0.28	0.62

*Loss on Ignition: 3.26; **Specific surface area (cm^2/g): 3635.

2.2. Synthesis of Reinforced Mortars

Mortar samples including CNTs and CMFs were fabricated according to the EN 196-1 standard, using Portland Cement CEM I 52.5 N as cementitious material. Regarding the piezoresistivity tests, prismatic test samples 40 mm x 40 mm x 160 mm in size with electrodes embedded into them were fabricated (in triplicates) (Figure 1). Concerning the conductivity tests, prismatic test samples 40 mm x 40 mm x 160 mm in size were prepared (in triplicates).

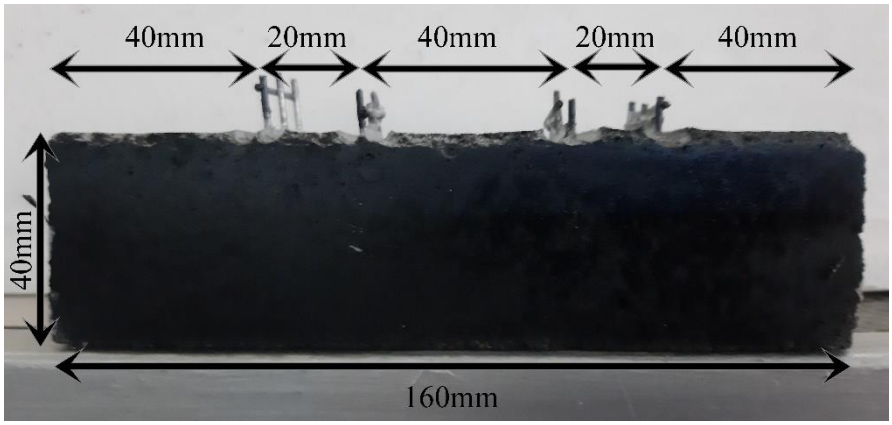

Figure 1. Indicative photo of prismatic test sample 40 mm x 40 mm x 160 mm in size with electrodes embedded into them.

The CNTs were incorporated into the aforementioned mixture as additives at several concentrations bwoc. In detail, the CNTs were added in a beaker containing the desired water (w/c = 0.5) and SIKA SI100 stabilizer (max. conc. 0.3% bwoc) under vigorous stirring with a magnetic stirrer. Subsequently, the suspension was subjected to ultrasonic treatment for 45 min and then was added into the stirring bowl together with cement powder, sand and silica fume. Prior to the preparation of the composite samples, the surface of the CNTs was functionalized by chemical modification introducing oxygen-containing groups such as hydroxyl (-OH), carboxyl (-COOH) and carbonyl (C=O) groups. This modification promoted the wettability of the CNTs and the bonding between their surfaces with the hydration products. The mortar was prepared by mechanical mixing and was compacted in a Teflon mold using a jolting apparatus. The specimens in the mold were kept at room temperature conditions for 24 h and then the demolded specimens were placed under water for a curing period of 28 days. Figure 2 illustrates the aforementioned synthetic procedure. According to the aforementioned procedure, CNT-reinforced mortar specimens, CMF-reinforced mortar specimens and CNT/CMF-reinforced mortar specimens were fabricated using the parameters tabulated in Table 2**,** Table 3 and Table 4, respectively.

 doi:10.20944/preprints202406.0937.v1

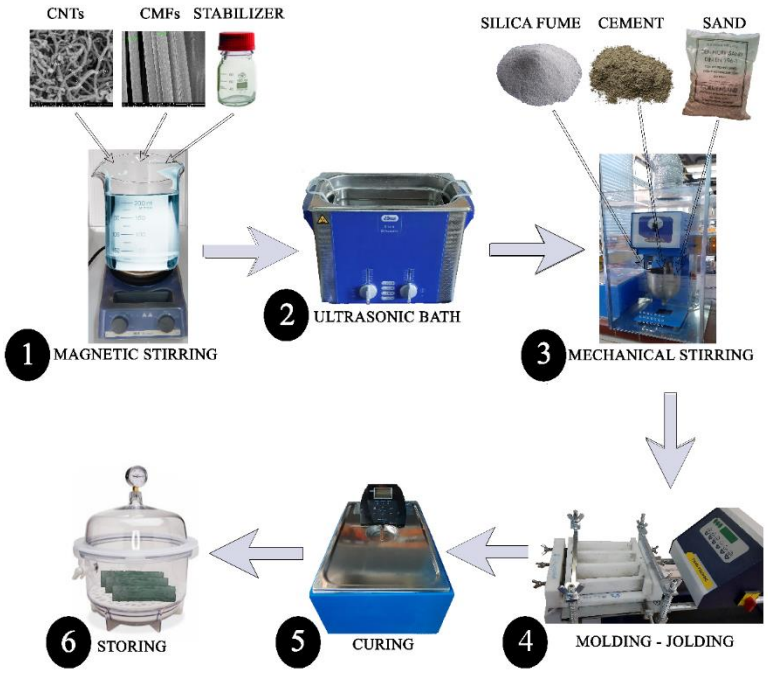

Figure 2. Schematic representation of the synthetic process for the fabrication of prismatic test samples: 40 mm x 40 mm x 160 mm in size.

The aim was to evaluate the influence of both CNTs and CMFs together with silica fume into the mortar specimens with respect to their mechanical and piezoresistive properties. Silica fume which was selected to be incorporated into the mortar specimens, improved the mechanical properties of the mortar due to the increase of the secondary hydrated reactions with $Ca(OH)_2$ resulting to the formation of C-S-H gel [18,20,33]. The chosen concentration of CMF for the fabrication of CNT/CMF-reinforced mortar specimens was 0.4% bwoc (Table 4) because the Mortar-0.4% CMF specimen demonstrated the best flexural strength value of all the CMF-reinforced mortar specimens (as it is discussed in detail in section 3.2. Mechanical properties).

Table 2. Tabulated parameters for the fabrication of CNT-reinforced mortar specimens using silica fume.

Samples	**Cement (g)**	**Silica fume (g)**	**Sand (g)**	**Ratio w/c**	**H_2O (ml)**	**Concentration CNTs (% bwoc)**	**Sika®Stabilizer-100 (g)**
Mortar-Ref	405	45	1350	0.5	225	-	-
Mortar-0.02% CNT	405	45	1350	0.5	225	0.02	0.25
Mortar-0.05% CNT	405	45	1350	0.5	225	0.05	0.625
Mortar-0.1% CNT	405	45	1350	0.7	315	0.1	1.25
Mortar-0.2% CNT	405	45	1350	0.7	315	0.2	2.5
Mortar-0.5% CNT	405	45	1350	0.7	315	0.5	6.25

Table 3. Tabulated parameters for the fabrication of CMF-reinforced mortar specimens using silica fume.

Samples	**Cement (g)**	**Silica fume (g)**	**Sand (g)**	**Ratio w/c**	**H_2O (ml)**	**Concentration CMFs (%bwoc)**	**Sika®Stabilizer-100 (g)**

 doi:10.20944/preprints202406.0937.v1

Mortar-Ref	405	45	1350	0.5	225	-	-
Mortar-0.05% CMF	405	45	1350	0.5	225	0.05	0.405
Mortar-0.2% CMF	405	45	1350	0.5	225	0.2	0.405
Mortar-0.25% CMF	405	45	1350	0.7	315	0.25	0.405
Mortar-0.3% CMF	405	45	1350	0.7	315	0.3	0.405
Mortar-0.4% CMF	405	45	1350	0.7	315	0.4	0.405
Mortar-1% CMF	405	45	1350	0.7	315	1	0.405

Table 4. Tabulated parameters for the fabrication of CNT/CMF-reinforced mortar specimens. For each sample 405 g of cement, 45 g of silica fume and 1350 g of sand were used, respectively.

Samples	**Ratio w/c**	**H_2O (ml)**	**Concentration CNTs (%bwoc)**	**Concentration CMFs (%bwoc)**	**Sika®Stabilizer-100 (g)**
Mortar-Ref	0.5	225	-	-	-
Mortar-0.4%CMFs+0.02%CNTs	0.5	225	0.02	0.04	0.225
Mortar-0.4%CMFs+0.05%CNTs	0.5	225	0.05	0.04	0.5625
Mortar-0.4%CMFs+0.1%CNTs	0.5	225	0.1	0.04	1.125

2.3. Characterization

The morphology of the additives and the mortar specimens was estimated via scanning electron microscopy (SEM) using a Hitachi Electron Microscope TM3030 coupled with an Ultra-High Resolution Scanning Electron Microscope (UHR-SEM) and a NOVA NANOSEM 230 (FEI Company, Hillsboro, United States, 2009) equipped with an Energy Dispersive X-Ray Spectrophotometer (EDS) (QUANTAX 70, BRUKER, Billerica, Massachusetts, United States, 2016).

The macro mechanical integrity was investigated by means of flexural strength (EN 196-1) using a material testing machine to apply loads (Instron 1121) with a displacement rate (speed) of 1 mm/min (Figure 3) and by means of compressive strength (EN 196-1) using a INSTRON 300DX-B1-C4-G6C with a displacement rate (speed) of 5 mm/min (Figure 4). It is mentioned that for the compressive strength tests, the specimens that were used were the prism halves from the flexural strength tests.

Figure 3. Flexural strength measurements.

 doi:10.20944/preprints202406.0937.v1

Figure 4. Compressive strength measurements.

The piezoresistive response properties of the aforementioned CNT-reinforced mortar specimens, CMF-reinforced mortar specimens and CNT/CMF-reinforced mortar specimens were evaluated using a data acquisition system via the four-probe method. The dimensions of the prismatic samples were 40 mm x 40 mm x 160 mm with stainless steel mesh electrodes embedded into them. The resistivity was measured as a function of cyclic load in order to evaluate the self-sensing properties of the produced mortar samples. The aim of using relative resistance measurement under cyclic loading is to monitor the material's sensing capability during a loading-unloading procedure. The electrical measurements were obtained using a Keithley Source-Meter 2400 together with a material testing machine applying loads (Instron 1121). In each measurement a fixed direct current (DC) of 1 mA was applied to the outer two electrical contacts while the voltage drop between the inner electrical contacts was measured (Figure 5). The displacement rate (speed) was 1 mm/min, the cyclic load ranged from 0.2 kN to 9.5 kN, (a pre-stress was applied equal to 0.2 kN) and a laser extensometer Fielder Optoelektronik K-100 was used to accurately measure the displacement measurement. Then, the relative change of the electrical resistance $\frac{(\Delta R)}{R_o}$ (fractional change in resistance, *FCR*) as a function of time was recorded under repeated compressive loading, where R_0 is the initial electrical resistance of specimens with compressive loading equal to 0.2 kN, at the beginning of the experiment. The results can be depicted either as a function of load or as a function of stress. In order to eliminate the effect of electric polarization and depolarization of cement-based materials on compressive sensitivity testing results, enough time was left to pass till the voltage value is stable. The resistivity ρ of the modified mortar sample is calculated by the equation (1):

$$\rho = \frac{RS}{l} \qquad (1)$$

where S is the effective area of voltage pole (the cross-sectional area), l the space between the two voltage poles (the length of the material being tested in the direction of the resistance R) and R is the electrical resistance [or volume (bulk) resistance].

Then, the *FCR* is given by the equation (2):

$$FCR = \frac{(\Delta R)}{R_o} = \frac{(\Delta \rho)}{\rho_o} + \left[\frac{(\Delta l)}{l_o}\right](1 + v_1 + v_2) \qquad (2)$$

where $\frac{(\Delta l)}{l_o}$ is the compressive strain and v_1 and v_2 are the values of the Poisson's ratio in the two transverse directions [34]. According to equation (2), ΔR depends on both $\Delta \rho$ and Δl. It is assumed that the resistance change is a display of the piezoresistivity, therefore $\frac{(\Delta \rho)}{\rho_o} >> \frac{(\Delta l)}{l_o}$, and subsequently, equation (2) becomes:

$$FCR = \frac{(\Delta R)}{R_o} = \frac{(\Delta \rho)}{\rho_o} \qquad (3)$$

 doi:10.20944/preprints202406.0937.v1

The effect of sensing of the inherent piezoresistivity (evaluation of the sensitivity of the strain sensor) is described by the gauge factor (*GF*), which is defined as the *FCR* per unit strain (equation 4). The GF constitutes a means of evaluation of the inherent piezoresistivity of a material, having exemplified the irreversible resistivity changes due to impairment or permanent microstructure alterations. In this work GF is determined via the four-probe method which as indicated in literature constitutes a safer and a more accurate approach compared to the two-probe method [34,35].

$$GF = \frac{\frac{(\Delta R)}{R_O}}{\frac{(\Delta l)}{l_o}} = \frac{\frac{(\Delta \rho)}{\rho_O}}{\frac{(\Delta l)}{l_o}} \quad (4)$$

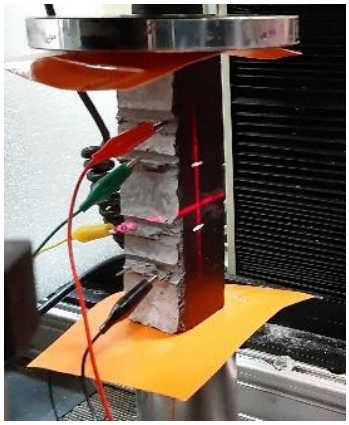

Figure 5. Indicative photo of the experimental setup for measuring the electrical resistance under compressive load of prismatic test samples: 40 mm x 40 mm x 160 mm in size.

3. Results

3.1. Morphological and Structural Characterization

The SEM images of the produced CNTs and the utilized CMFs are illustrated in Figure 6 and Figure 7, respectively. In the case of the produced CNTs the SEM image reveals that they are tangled, and are distributed randomly. They appear in varying sizes and their diameter ranges between 14 and 45 nm. In the case of the CMFs, the SEM image depicts that their diameter is roughly 6.9 ± 0.2 μm.

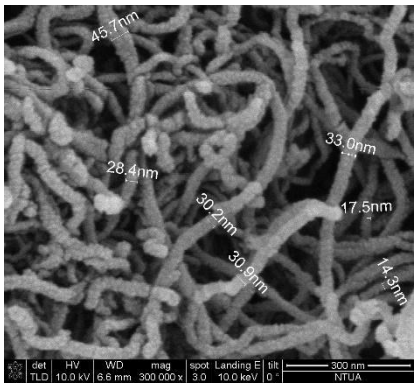

Figure 6. The SEM image of the produced MWCNTs (x 300,000).

 doi:10.20944/preprints202406.0937.v1

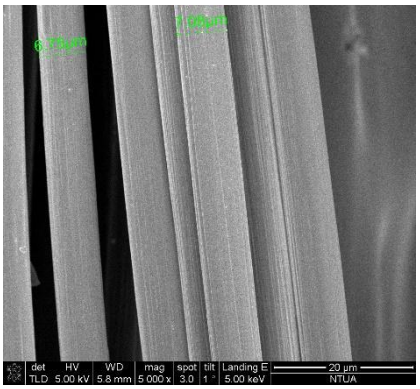

Figure 7. The SEM image of the utilized CMFs (x 5,000).

Moreover, the SEM images of mortars with incorporated CNTs and CMFs are depicted in Figures 8–11.

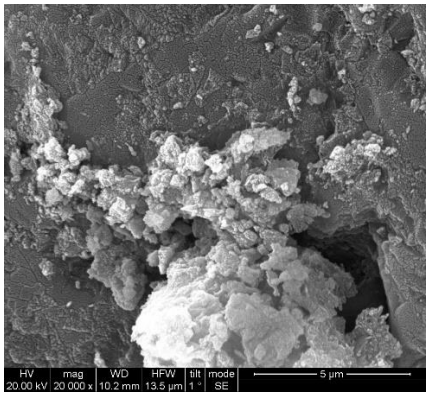

Figure 8. SEM image of Mortar-Reference.

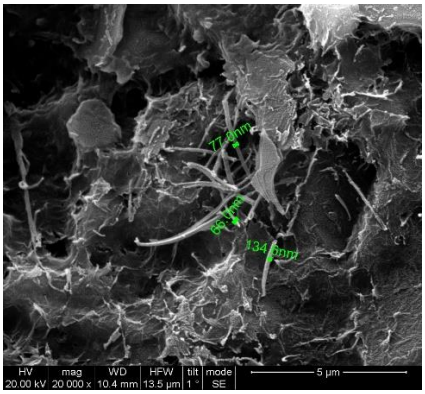

Figure 9. SEM image of Mortar-0.4%CMFs+0.02%CNTs.

 doi:10.20944/preprints202406.0937.v1

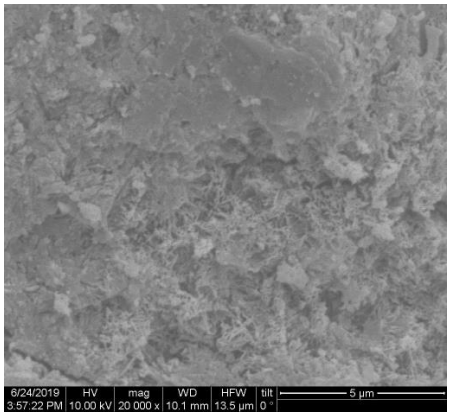

Figure 10. SEM image of Mortar-0.4%CMFs+0.05%CNTs.

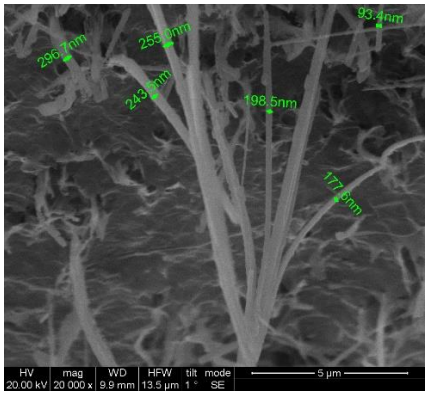

Figure 11. SEM image of Mortar-0.4%CMFs+0.1%CNTs.

All SEM images illustrated in Figures 8–11 are 20,000x magnified. In the specimens of Mortar-0.4%CMFs+0.02%CNTs and Mortar-0.4%CMFs+0.1%CNTs, the presence and the dispersion of CMFs and CNTs is clearly observed. Moreover, their diameter can be determined in some cases, ranging for CMFs from 134 nm to around 300 nm and for CNTs from 66 nm to 94 nm. For the case of Mortar-0.4%CMFs+0.05%CNTs the picture resolution did not allow such measurements. Additionally, it is depicted that CMFs and CNTs are tangled and randomly distributed within the bulk mortar specimen.

3.2. Mechanical Properties

The obtained values of the flexural and compressive strength of reference specimens, as well as CNT-, CMF- and CNT/CMF-reinforced mortar specimens are depicted in Figures 12–17. All specimens were evaluated after 28 days of curing in water.

Figures 12 and 13 demonstrate the flexural and compressive strength of CNT-reinforced mortar specimens. Taking into account these results, it may be remarked that the highest flexural strength as well as compressive strength values are demonstrated for the sample with 0.05% CNTs bwoc.

Preprints.org (www.preprints.org) | NOT PEER-REVIEWED | Posted: 13 June 2024 doi:10.20944/preprints202406.0937.v1

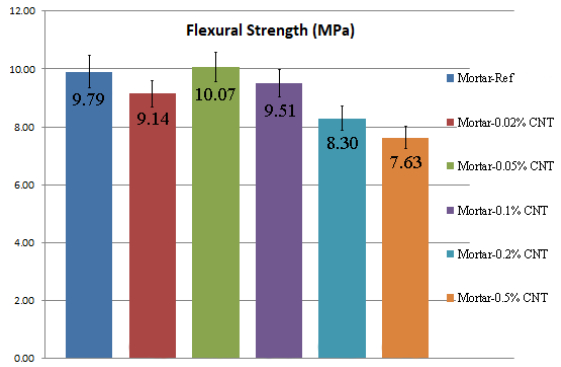

Figure 12. The flexural strength of CNT-reinforced mortar specimens.

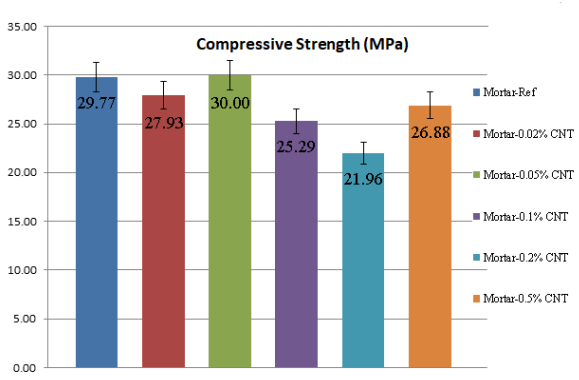

Figure 13. The compressive strength of CNT-reinforced mortar specimens.

Figures 14 and 15 demonstrate the flexural and compressive strength measurements of CMF-reinforced mortar specimens. Taking into account these results, it may be remarked that the incorporation of CMFs into the mortar does not enhance the flexural strength properties of the composites. However, the best flexural strength value was depicted for the sample with 0.4% CMFs bwoc. On the other hand, the incorporation of CMFs into the mortar enhances the compressive strength properties of the composites for all CMFs concentration. The sample with 0.2% CMFs bwoc demonstrated the highest compressive strength value.

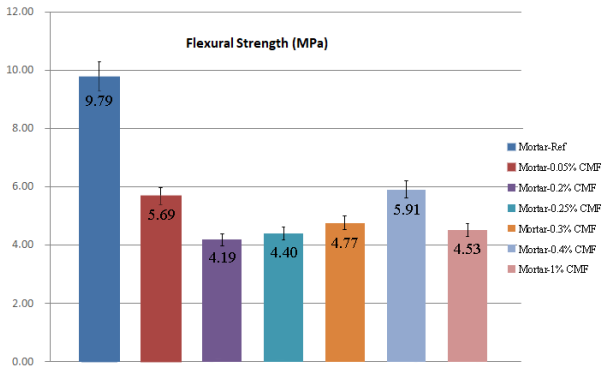

Figure 14. The flexural strength of CMF-reinforced mortar specimens.

 doi:10.20944/preprints202406.0937.v1

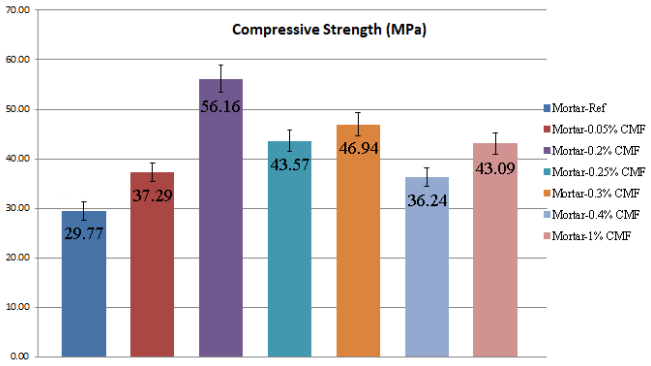

Figure 15. The compressive strength of CMF-reinforced mortar specimens.

Figures 16 and 17 demonstrate the flexural and compressive strength measurements of CNT/CMF-reinforced mortar specimens. Taking into account these results, it can be seen that the incorporation of both CNTs and CMFs into the mortar influences the flexural strength of the composites. Moreover, the sample with 0.4% CMFs and 0.05% CNTs bwoc exhibits the highest flexural strength values. On the other hand, it is clearly denoted that the incorporation of both CNTs and CMFs into the mortar enhances the compressive strength of the composites. Furthermore, the sample with 0.4% CMFs and 0.05% CNTs bwoc exhibits the highest compressive strength value.

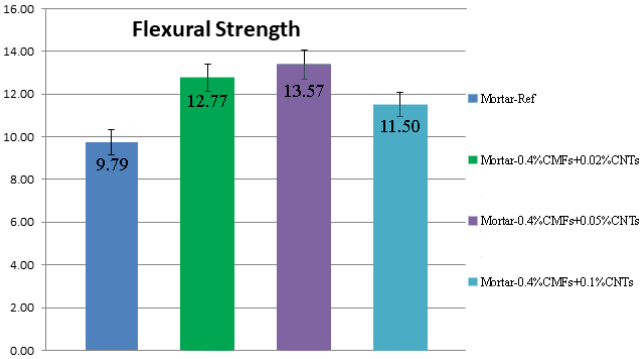

Figure 16. The flexural strength of CNT/CMF-reinforced mortar specimens.

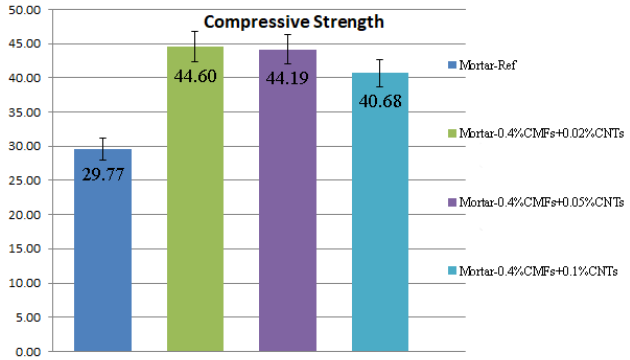

Figure 17. The compressive strength of CNT/CMF-reinforced mortar specimens.

Taking into account all the above-mentioned results, it can be seen that the incorporation of both CNTs and CMFs into the mortar influences the flexural strength of the composites. The maximum flexural strength was reported in the case of the mortar reinforced with 0.4% CMFs and 0.05% CNTs bwoc, which showed an increment of 36.57% compared to the control specimens. Another specimen

 doi:10.20944/preprints202406.0937.v1

that showed improved flexural strength by 30.44% compared to the mortar-reference was the mortar reinforced with 0.4% CMFs and 0.02% CNTs bwoc. In the cases of mortars reinforced only with CNTs or only with CMFs their flexural strength was degraded compared to the mortar-reference samples. In the case of reinforced mortars only with CNTs, this behavior is attributed to the poor dispersion of CNTs in the cementitious matrix. On the other hand, in the case of mortars reinforced only with CMFs the flexural strength degradation apart from the poor CMFs dispersion is probably owed to the fact that CMFs short length leads to the failure in load transfer [35,36]. On the contrary, when mortars are reinforced with both CNTs and CMFs the increment in flexural strength suggests a better CNTs dispersion in the cementitious matrix owed to the presence of the CMFs.

As indicated also by these results, compressive strength of mortars is also affected by the presence of CNTs and CMFs. The mortar specimens reinforced with only CMFs and CNTs/CMFs showed improved compressive strength for all CMFs and CNTs/CMFs concentrations compared to the mortar-reference specimen. The maximum compressive strength was reported in the case of the mortar reinforced with 0.2% CMFs bwoc, which showed an increment of 88.65% compared to the control specimens. CMFs due to their low specific surface area do not absorb water during the mixing procedure, thus not negatively influencing the cement paste workability. Moreover, their high flexibility prevents fibers interlocking, something that is common for stiff reinforcement bars such as steel bars. As a result, CMFs reinforced mortars show improved compressive strength compared to reference specimens. On the other hand, the mortar specimens when only CNTs were incorporated in them, revealed degradation in their compressive strength. This is attributed to poor CNTs dispersion in the cementitious matrix as also mentioned earlier in the evaluation of the corresponding mortars flexural strength.

Finally, it must be mentioned that the compressive strength of the reference samples was determined below the expected 52.5 MPa because of poorly controlled curing conditions and more specifically, low temperature and humidity during the first day of curing and low temperature during the rest curing days.

3.3. Self-Sensing Capacity

Taking into account the optimum mechanical performance of the CNT/CMF-reinforced mortar composites with regard to flexural and compressive strength, the cases of mortar-0.4%CMF+0.02%CNTs and mortar-0.4%CMF+0.05%CNTs were chosen to be examined for their self-sensing capacity.

Results of the piezoresistive response of reference mortar and the above-mentioned mortar composite specimens are illustrated in the following Figures 18–23. Piezoresistivity is a means of evaluating the sensing of changes in stress and/or strain via the measurement of electrical resistance.

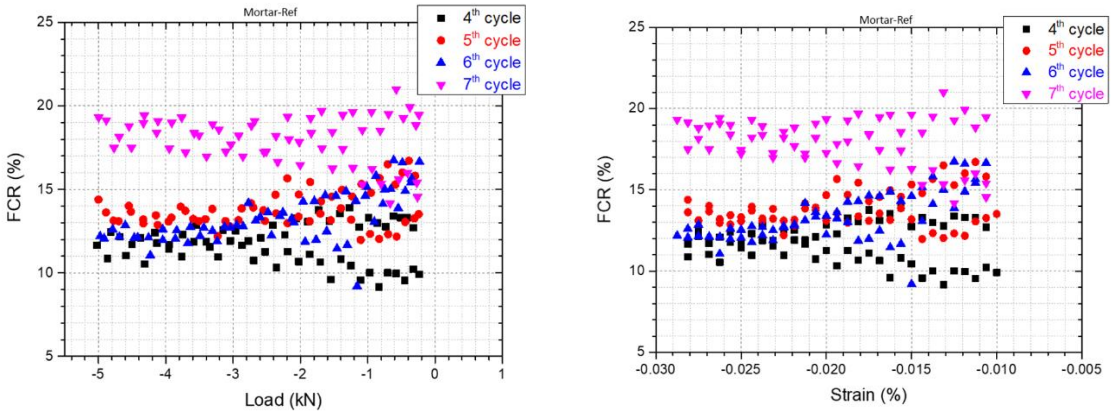

Figure 18. Fractional Change of resistivity vs (a)- inflicted load, (b)-inflicted strain for mortar reference specimens.

 doi:10.20944/preprints202406.0937.v1

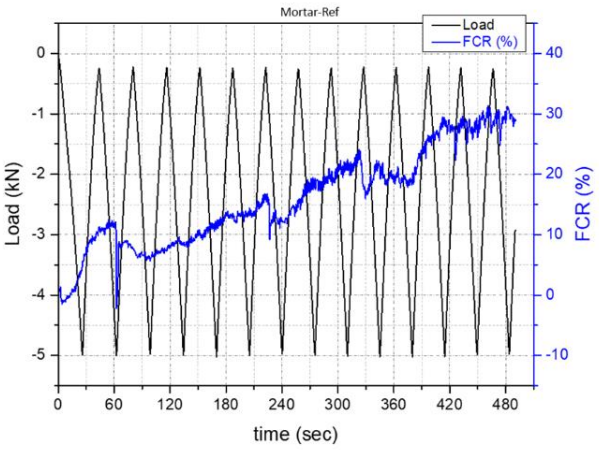

Figure 19. Fractional changes of resistivity for mortar reference specimens.

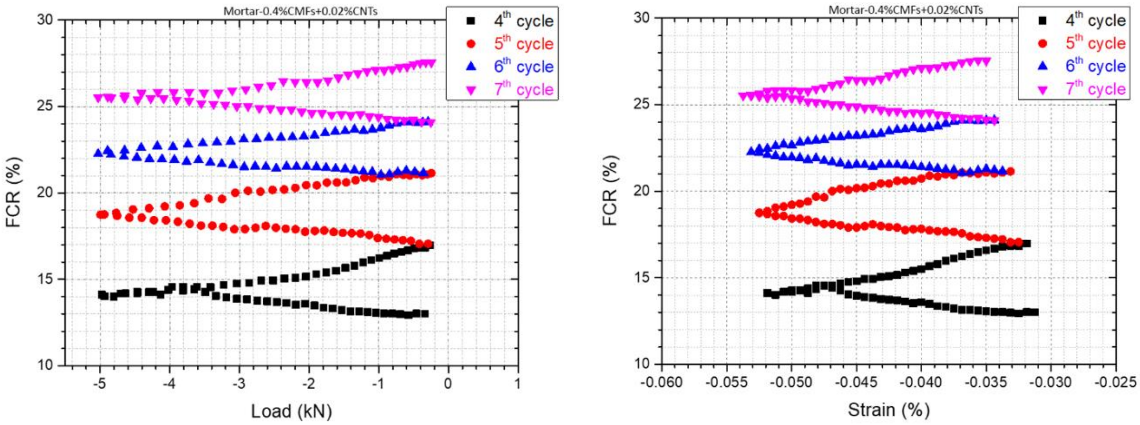

Figure 20. Fractional Change of resistivity vs (a)- inflicted load, (b)-inflicted strain for mortar-0.4%CMF+0.02%CNTs specimens.

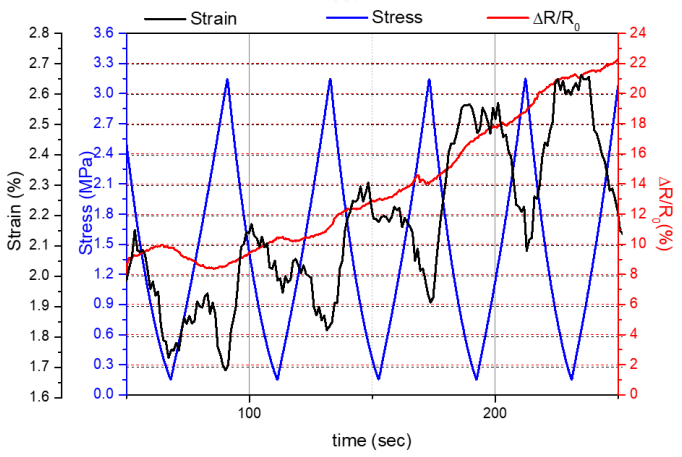

Figure 21. Fractional changes of resistivity for mortar-0.4%CMF+0.02%CNTs specimens.

 doi:10.20944/preprints202406.0937.v1

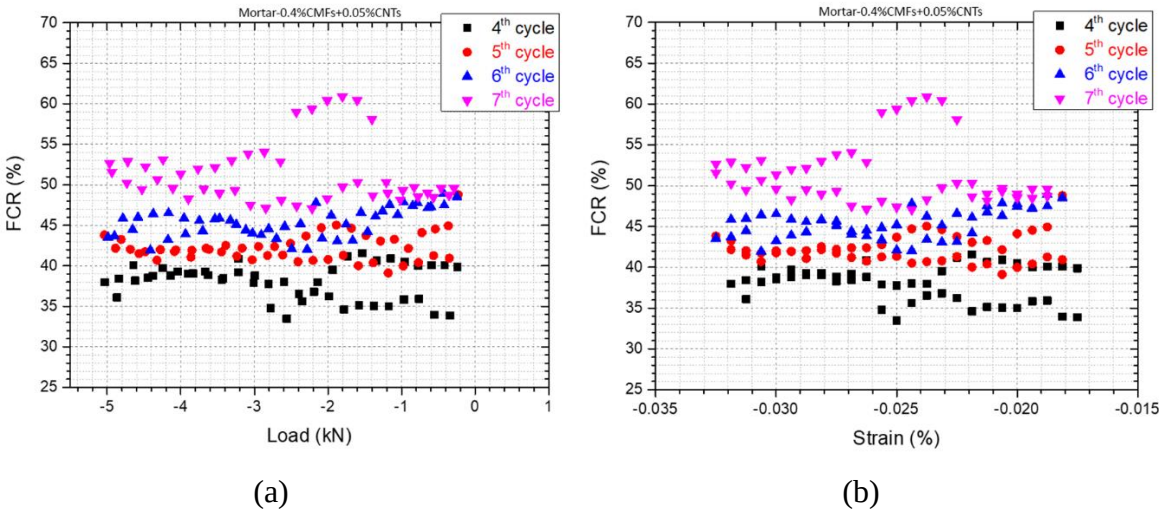

Figure 22. Fractional Change of resistivity vs (a)- inflicted load, (b)-inflicted strain for mortar-0.4%CMF+0.05%CNTs specimens.

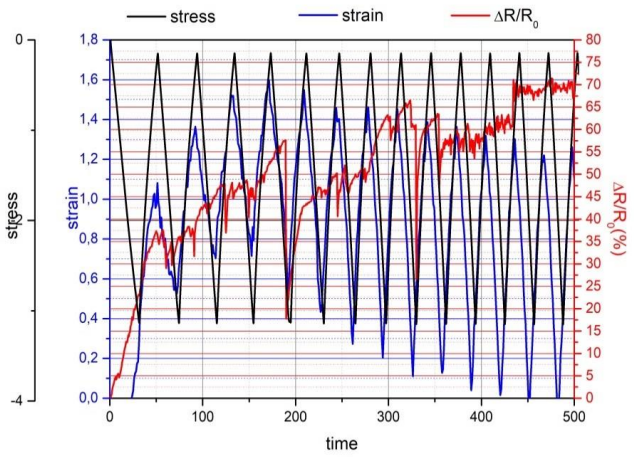

Figure 23. Fractional changes of resistivity for mortar-0.4%CMF+0.05%CNTs specimens.

The graphs reflect the compression loading – unloading cycles and the corresponding FCR under the infliction of DC. The loading and strain values are negative since the mortar specimens are compressed during the tests. It can be clearly seen from the above diagrams depicting the piezoresistivity response of the received specimens that the DC current used, causes severe polarization effect since there is a constant increase in the resistivity/resistance over time. This phenomenon has been thoroughly highlighted and discusssed also in literature [37]. The electrical polarization caused by the movement and aggregation of ions, changes the electrical conduction mechanism, which is dominated, in this case, by the ionic conduction. As a result, the measured resistance is extremely increased, making it difficult to determine the changes in resistance during cyclic compressive loading during DC measurement. To overcome this pitfall, the DC is applied for some time before the infliction of the compression loading. In this way the system total resistance becomes stable and the polarization effect is neutralized [38].

Moreover, it should be mentioned that the gradual increase in baseline resistance as stress cycling progressed can be attributed to irreversible damage in the mortar specimens. The increase in the amplitude of resistance variation as cycling progresses is attributed to the effect of damage on the extent of defect dynamics. The greater the damage, the greater the extent of defect healing during loading and the greater the extent of defect aggravation during unloading [39]. In the regime of elastic deformation, the damage does not affect the strain permanently, as shown by the total reversibility

 doi:10.20944/preprints202406.0937.v1

of the strain during cyclic loading. Nevertheless, damage occurs during stress increase, causing a damage-induced resistance increase. The damage-induced resistance increase is a sensitive indicator of minor damage (without a change in modulus), in addition to being a sensitive indicator of major damage (with a decrease in modulus). In contrast, the intense and abrupt baseline resistance increase is an indicator of major damage only, which is not apparent here [39]. It should also be noted that the strain does not return to zero at the end of each cycle, denoting that the specimen is subjected to plastic deformation and subsequent crack formation.

Based on the analysis above and taking into consideration Figure 19, Figure 21 and Figure 23, the fractional change of resistivity for the mortar reference and the mortar-0.4%CMF+0.02%CNTs samples, respectively, exhibits a steep increase which is attributed to damages induced to the mortar specimens during the cycles of loading – unloading owed to the inherent brittleness of the material. On the contrary, a smoother increase in the fractional change of resistivity as well as the fact that this change seems to be reversible upon loading (increase of stress) as depicted in the case of the mortar-0.4%CMF+0.05%CNTs samples (Figure 23), comprise strong indications that the composites with the specific loads of CMF and CNTs have attained a self-responsive behavior.

The maximum value of GF determined during the cycles of loading-unloading for the mortar composite samples (0.4%CMF+0.02%CNTs and 0.4%CMF+0.05%CNTs) are shown in Table 5 below.

Table 5. Maximum GF for self-sensing additives content.

CMF+CNTs (%)	GF (maximum)
0.4 + 0.02	959
0.4 + 0.05	4980

In literature, GF values for cementitious materials are reported to be below 500 even below 100 even in the cases of the incorporation of nanofillers and/or continuous fibers [35]. On the contrary, GF values determined in this work fall under the category of “giant piezoresistivity”, since they are greater than 500. This behavior is attributed to two separate mechanisms, the first one due to the incorporation of CNTs as conductive nanoparticulates and the second one due to the incorporation of CMF which are discontinuous fibers and more specifically discontinuous carbon fibers which are also conductive. As far as the first mechanism is concerned, when tension is induced, proximity of CNTs nanoparticles is improved in the cementitious composite thus reducing its resistivity and consequently increasing its GF value. In the case of improving the proximity of nanoparticles to the extent of creating a continuous conductive path, the reduction of the resistivity is greatly enhanced and so is the increase of the GF value, while the concentration of the nanoparticles in the composite is acknowledged as the percolation threshold. As for the second mechanism, the incorporation of discontinuous carbon fibers (CMF) tends to bridge microcracks formed in the brittle cementitious matrix. Upon tension application the fibers, the width of microcracks becomes larger and a pull-out effect is observed in CMF, thus leading to resistivity increase and a subsequent GF reduction. On the contrary, when the tension seizes to exist, the pull-out effect is reversed and as a result the composite resistivity is reduced and the GF value is increased [35].

5. Conclusions

Structural materials with self-sensing and electrical actuation related properties have attracted considerable scientific attention over the past decades since such materials can contribute to sustainability in the construction sector and enhance safety within the life of constuctions. This work aims to contribute to the progress acceleration of these materials. The results attained constitute a solid groundwork in this direction. More specifically, it is shown that when CNTs and CMF are incorporated as admixtures in mortars, the composite materials show improved mechanical strength. Different concentrations of CNTs and CMF were evaluated, while the composites containing 0.4% bwoc CMF together with 0.02% and 0.05% bwoc CNTs stood out as the optimum ones in terms of flexural and compressive strength. These two cases of mortar composites, 0.4%CMF+0.02%CNTs and 0.4%CMF+0.05%CNTs, were then evaluated in terms of piezoresistivity. The results demonstrate that

 doi:10.20944/preprints202406.0937.v1

the percolation threshold of CMF/CNTs is 0.4%CMF+0.05%CNTs since this is the case with the highest GF value (4980) and the FCR present a smooth and reversible increase over time during loading and unloading cycles.

Author Contributions: Conceptualization, I.A.Kar. and E.K.K.; methodology, I.A.Kar., I.A.Kan. and A.I.C.; software, I.A.Kar., E.K.K. and I.A.Kan.; validation, I.A.Kar., E.K.K. and A.I.C.; formal analysis, I.A.Kar. and I.A.Kan; investigation, I.A.Kar. and A.I.C.; resources, I.A.Kar. and A.I.C.; data curation, I.A.Kar. and E.K.K.; writing—original draft preparation, I.A.Kar., I.A.Kan and E.K.K.; writing—review and editing, I.A.Kar. and C.A.C.; visualization, I.A.Kar. and C.A.C.; supervision, C.A.C.; project administration, C.A.C.; funding acquisition, C.A.C. All authors have read and agreed to the published version of the manuscript.

Funding: These results are part of the project that has received funding from the European Unions' HORIZON 2020 research and innovation program under grant agreement no. 685445 (LORCENIS).

Conflicts of Interest: The authors declare no conflict of interest.

References

1. Yang, G.; Zhao, J.; Wang, Y. Durability properties of sustainable alkali-activated cementitious materials as marine engineering material: a review. *Materials Today Sustainability* **2021**, 100099, doi:10.1016/j.mtsust.2021.100099.
2. Ramezani, M.; Dehghani, A.; Sherif, M.M. Carbon nanotube reinforced cementitious composites: A comprehensive review. *Construction and Building Materials* **2022**, *315*, 125100, doi:10.1016/j.conbuildmat.2021.125100.
3. Mittal, G.; Rhee, K.Y. Chemical vapor deposition-based grafting of CNTs onto basalt fabric and their reinforcement in epoxy-based composites. *Composites Science and Technology* **2018**, *165*, 84-94, doi:10.1016/j.compscitech.2018.06.018.
4. Hamzaoui, R.; Bennabi, A.; Guessasma, S.; Khelifa, R.; Leklou, N. Optimal Carbon Nanotubes Concentration Incorporated in Mortar and Concrete. *Advanced Materials Research* **2012**, *587*, 107-110, doi:10.4028/www.scientific.net/AMR.587.107.
5. Silvestro, L.; Jean Paul Gleize, P. Effect of carbon nanotubes on compressive, flexural and tensile strengths of Portland cement-based materials: A systematic literature review. *Construction and Building Materials* **2020**, *264*, 120237, doi:10.1016/j.conbuildmat.2020.120237.
6. Abu Al-Rub, R.K.; Tyson, B.M.; Yazdanbakhsh, A.; Grasley, Z. Mechanical Properties of Nanocomposite Cement Incorporating Surface-Treated and Untreated Carbon Nanotubes and Carbon Nanofibers. *Journal of Nanomechanics and Micromechanics* **2012**, *2*, 1-6, doi:10.1061/(asce)nm.2153-5477.0000041.
7. Evangelista, A.C.J.; de Morais, J.F.; Tam, V.; Soomro, M.; Torres Di Gregorio, L.; Haddad, A.N. Evaluation of Carbon Nanotube Incorporation in Cementitious Composite Materials. *Materials (Basel)* **2019**, *12*, doi:10.3390/ma12091504.
8. Li, X.; Rafieepour, S.; Miska, S.Z.; Takach, N.E.; Ozbayoglu, E.; Yu, M.; Mata, C. Carbon nanotubes reinforced lightweight cement testing under tri-axial loading conditions. *Journal of Petroleum Science and Engineering* **2019**, *174*, 663-675, doi:10.1016/j.petrol.2018.11.077.
9. Chen, S.J.; Collins, F.G.; Macleod, A.J.N.; Pan, Z.; Duan, W.H.; Wang, C.M. Carbon nanotube–cement composites: A retrospect. *The IES Journal Part A: Civil & Structural Engineering* **2011**, *4*, 254-265, doi:10.1080/19373260.2011.615474.
10. de Souza, T.C.; Pinto, G.; Cruz, V.S.; Moura, M.; Ladeira, L.O.; Calixto, J.M. Evaluation of the rheological behavior, hydration process, and mechanical strength of Portland cement pastes produced with carbon nanotubes synthesized directly on clinker. *Construction and Building Materials* **2020**, *248*, 118686, doi:10.1016/j.conbuildmat.2020.118686.

11. Jung, M.; Lee, Y.-s.; Hong, S.-G.; Moon, J. Carbon nanotubes (CNTs) in ultra-high performance concrete (UHPC): Dispersion, mechanical properties, and electromagnetic interference (EMI) shielding effectiveness (SE). *Cement and Concrete Research* **2020**, *131*, 106017, doi:10.1016/j.cemconres.2020.106017.
12. Gao, J.; Sha, A.; Wang, Z.; Hu, L.; Yun, D.; Liu, Z.; Huang, Y. Characterization of carbon fiber distribution in cement-based composites by Computed Tomography. *Construction and Building Materials* **2018**, *177*, 134-147, doi:10.1016/j.conbuildmat.2018.05.114.
13. Chuang, W.; Geng-sheng, J.; Bing-liang, L.; Lei, P.; Ying, F.; Ni, G.; Ke-zhi, L. Dispersion of carbon fibers and conductivity of carbon fiber-reinforced cement-based composites. *Ceramics International* **2017**, *43*, 15122-15132, doi:10.1016/j.ceramint.2017.08.041.
14. Díaz, B.; Guitián, B.; Nóvoa, X.R.; Pérez, C. Analysis of the microstructure of carbon fibre reinforced cement pastes by impedance spectroscopy. *Construction and Building Materials* **2020**, *243*, 118207, doi:10.1016/j.conbuildmat.2020.118207.
15. Tong, Z.; Guo, H.; Gao, J.; Wang, Z. A novel method for multi-scale carbon fiber distribution characterization in cement-based composites. *Construction and Building Materials* **2019**, *218*, 40-52, doi:10.1016/j.conbuildmat.2019.05.115.
16. Kim, G.M.; Park, S.M.; Ryu, G.U.; Lee, H.K. Electrical characteristics of hierarchical conductive pathways in cementitious composites incorporating CNT and carbon fiber. *Cement and Concrete Composites* **2017**, *82*, 165-175, doi:10.1016/j.cemconcomp.2017.06.004.
17. Yoon, H.N.; Jang, D.; Lee, H.K.; Nam, I.W. Influence of carbon fiber additions on the electromagnetic wave shielding characteristics of CNT-cement composites. *Construction and Building Materials* **2021**, *269*, 121238, doi:10.1016/j.conbuildmat.2020.121238.
18. Fang, Y.; Wang, J.; Ma, H.; Wang, L.; Qian, X.; Qiao, P. Performance enhancement of silica fume blended mortars using bio-functionalized nano-silica. *Construction and Building Materials* **2021**, *312*, 125467, doi:10.1016/j.conbuildmat.2021.125467.
19. Chen, H.; Chen, Q.; Xu, Y.; Lawi, A.S. Effects of silica fume and Fly ash on properties of mortar reinforced with recycled-polypropylene. *Construction and Building Materials* **2022**, *316*, 125887, doi:10.1016/j.conbuildmat.2021.125887.
20. Song, C.; Hong, G.; Choi, S. Effect of dispersibility of carbon nanotubes by silica fume on material properties of cement mortars: Hydration, pore structure, mechanical properties, self-desiccation, and autogenous shrinkage. *Construction and Building Materials* **2020**, *265*, 120318, doi:10.1016/j.conbuildmat.2020.120318.
21. Kim, G.M.; Nam, I.W.; Yang, B.; Yoon, H.N.; Lee, H.K.; Park, S. Carbon nanotube (CNT) incorporated cementitious composites for functional construction materials: The state of the art. *Composite Structures* **2019**, *227*, 111244, doi:10.1016/j.compstruct.2019.111244.
22. Kim, H.K.; Nam, I.W.; Lee, H.K. Enhanced effect of carbon nanotube on mechanical and electrical properties of cement composites by incorporation of silica fume. *Composite Structures* **2014**, *107*, 60-69, doi:10.1016/j.compstruct.2013.07.042.
23. Stynoski, P.; Mondal, P.; Marsh, C. Effects of silica additives on fracture properties of carbon nanotube and carbon fiber reinforced Portland cement mortar. *Cement and Concrete Composites* **2015**, *55*, 232-240, doi:10.1016/j.cemconcomp.2014.08.005.
24. Lee, S.J.; You, I.; Zi, G.; Yoo, D.Y. Experimental Investigation of the Piezoresistive Properties of Cement Composites with Hybrid Carbon Fibers and Nanotubes. *Sensors (Basel)* **2017**, *17*, doi:10.3390/s17112516.

25. Garg, M.; Das, C.S.; Gupta, R. Use of silica particles to improve dispersion of -COOH CNTs/carbon fibers to produce HyFRCC. *Construction and Building Materials* **2020**, *250*, 118777, doi:10.1016/j.conbuildmat.2020.118777.
26. Kim, G.M.; Yoon, H.N.; Lee, H.K. Autogenous shrinkage and electrical characteristics of cement pastes and mortars with carbon nanotube and carbon fiber. *Construction and Building Materials* **2018**, *177*, 428-435, doi:10.1016/j.conbuildmat.2018.05.127.
27. Zhan, M.; Pan, G.; Zhou, F.; Mi, R.; Shah, S.P. In situ-grown carbon nanotubes enhanced cement-based materials with multifunctionality. *Cement and Concrete Composites* **2020**, *108*, 103518, doi:10.1016/j.cemconcomp.2020.103518.
28. Zhou, Z.; Xie, N.; Cheng, X.; Feng, L.; Hou, P.; Huang, S.; Zhou, Z. Electrical properties of low dosage carbon nanofiber/cement composite: Percolation behavior and polarization effect. *Cement and Concrete Composites* **2020**, *109*, 103539, doi:10.1016/j.cemconcomp.2020.103539.
29. Ding, S.; Ruan, Y.; Yu, X.; Han, B.; Ni, Y.-Q. Self-monitoring of smart concrete column incorporating CNT/NCB composite fillers modified cementitious sensors. *Construction and Building Materials* **2019**, *201*, 127-137, doi:10.1016/j.conbuildmat.2018.12.203.
30. Collins, F.; Lambert, J.; Duan, W.H. The influences of admixtures on the dispersion, workability, and strength of carbon nanotube–OPC paste mixtures. *Cement and Concrete Composites* **2012**, *34*, 201-207, doi:10.1016/j.cemconcomp.2011.09.013.
31. Goulis, P.; Kartsonakis, I.A.; Mpalias, K.; Charitidis, C. Combined effects of multi-walled carbon nanotubes and lignin on polymer fiber-reinforced epoxy composites. *Materials Chemistry and Physics* **2018**, *218*, 18-27, doi:10.1016/j.matchemphys.2018.07.025.
32. Trompeta, A.-F.A.; Koumoulos, E.P.; Kartsonakis, I.A.; Charitidis, C.A. Advanced characterization of by-product carbon film obtained by thermal chemical vapor deposition during CNT manufacturing. *Manufacturing Review* **2017**, *4*, 7, doi:10.1051/mfreview/2017006.
33. Luo, T.; Hua, C.; Sun, Q.; Tang, L.; Yi, Y.; Pan, X. Early-Age Hydration Reaction and Strength Formation Mechanism of Solid Waste Silica Fume Modified Concrete. *Molecules* **2021**, *26*, doi:10.3390/molecules26185663.
34. Deborah D. L. Chung, Functional Materials: Electrical, Dielectric, Electromagnetic, Optical and Magnetic Applications (Engineering Materials for Technological Needs), Singapore ; Hackensack, NJ : World Scientific, 2010.
35. Chung, D.D.L. A critical review of piezoresistivity and its application in electrical-resistance-based strain sensing. *Journal of Materials Science* **2020**, *55*, 15367-15396, doi:10.1007/s10853-020-05099-z.
36. Cwirzen, A.; Habermehl-Cwirzen, K. The Effect of Carbon Nano- and Microfibers on Strength and Residual Cumulative Strain of Mortars Subjected to Freeze-Thaw Cycles. *Journal of Advanced Concrete Technology* **2013**, *11*, 80-88, doi:10.3151/jact.11.80.
37. Han, B.; Yu, X.; Ou, J. Measurement of Sensing Signal of Self-Sensing Concrete. **2014**, 67-93, doi:10.1016/b978-0-12-800517-0.00004-6.

 doi:10.20944/preprints202406.0937.v1

38. Han, B.; Ding, S.; Yu, X. Intrinsic self-sensing concrete and structures: A review. *Measurement* **2015**, *59*, 110-128, doi:10.1016/j.measurement.2014.09.048.
39. Chung, D. Damage in cement-based materials, studied by electrical resistance measurement. *Materials Science and Engineering: R: Reports* **2003**, *42*, 1-40, doi:10.1016/s0927-796x(03)00037-8.